JOURNAL OF MATERIALS SCIENCE 29 (1994) 5475–5480

Sintering of MgO and MgO–TiC ceramics by plasma, microwave and conventional heating

M. BENGISU, O. T. INAL
New Mexico Institute of Mining and Technology, Materials and Metallurgical Engineering Department, Socorro, NM 87801, USA

The densification of MgO and MgO–TiC ceramics by hollow cathode plasma and microwave sintering techniques was studied. The resultant fractional densities were compared to those of conventionally sintered samples. It was demonstrated that indirect heating and sintering of MgO by microwave radiation was possible. Higher fractional densities were obtained in MgO by microwave sintering in comparison to conventional sintering under the same conditions. In the case of MgO–TiC composites, chemical reaction led to Mg_2TiO_4 formation in all samples. Plasma sintering suppressed this reaction and exhibited reduced sinterability upon TiC addition. On the other hand, small amounts of TiC additions aided the conventional sintering of MgO, resulting in better mechanical properties. Furthermore, commercial grade MgO was sintered to higher densities than relatively pure research grade MgO. Hardness and fracture toughness values are reported.

1. Introduction

MgO is a ceramic material with many potential applications owing to its high melting point (2620 °C), high resistivity ($> 10^{14}$) and good corrosion resistance [1, 2]. MgO has only one structure type at all temperatures up to its melting point. Above 1600 °C it is ductile, which can be used to advantage. Another very important advantage regarding MgO is its affordability and availability [2]. The main disadvantages of this material are its low fracture toughness [3] (2–3 $MPam^{1/2}$) and strength [1] (flexural strength about 100 MPa) and relatively slow sintering kinetics [4]. It is difficult to fully densify MgO without hot-pressing or the use of additives [4]. It has been shown for some oxide ceramics that novel techniques, such as microwave [5] and plasma sintering [6], provide increased densification rates or reduced sintering temperatures. To the author's knowledge no reports on attempting to sinter MgO and its composites by these techniques have appeared in the literature.

The aim of this study was to analyse the densification behaviour of MgO and MgO–TiC composites under microwave, plasma and conventional (resistive) heating and to compare the resultant microstructures and properties.

2. Experimental procedure

2.1. Preconsolidation processing

The starting materials were 99.5% pure MgO (MgO_p), technical grade MgO (MgO_{TG}) containing 98% MgO, 0.8% CaO, 0.35% SiO_2, 0.2% Fe_2O_3, 0.15% Al_2O_3 and 0.4% other impurities, and 99.5% pure TiC. Average Fisher particle sizes given by the manufacturers were 0.28, 5.00 and 1.56 μm, respectively. MgO–10 vol % TiC (MgO–10TiC) mixtures were prepared by ball milling in methanol for 5 h. Mixed slurries were partially dried on a hot plate while stirring. Further drying was achieved in a furnace at 100–200 °C for 10–15 min. This method prevented segregation of the different phases. Dried cakes were crushed and ground using an alumina pestle and mortar. The powders were screened using a 175 mesh sieve. MgO–10TiC powders, prepared by the above method, as well as MgO_p and MgO_{TG} powders, were dry-pressed at 19 MPa. Graphite foil was used to prevent sticking of pure MgO-containing powders to the top and bottom of the steel mould during cold-pressing.

Slips of each composition were prepared for slip casting by mechanical stirring of the constituents at high speed using a 3-speed household mixer. Since MgO reacts with water, alcohol is recommended for its slip casting [7]. Ethanol was used with MgO_p, while methanol was found to provide better dispersion of MgO_{TG}. In the case of MgO_p and MgO_p–10TiC powders, a solid:liquid ratio of 80% was used. However, a solid:liquid ratio of 150% was possible in the case of MgO_{TG} and MgO_{TG}–10TiC powders, probably due to the larger particle size, and thus, the smaller surface area that needed wetting. Preliminary experiments with slip casting of alcohol-based slurries indicated that cracking occurred due to high drying rates. Therefore, drying rates were reduced by covering the moulds. This allowed drying of 30 mm diameter by 10 mm thick samples in about 36 h. Slow drying totally eliminated the cracking problem.

Both cold-pressed and slip-cast MgO_p-containing bodies had low green densities compared to MgO_{TG}-containing bodies; 29% theoretical density (TD) ver-

0022–2461

sus 32–35% TD in the case of cold-pressed samples and 20% versus 25% TD in the case of slip-cast samples. Rods 6 mm in diameter and 20 mm in length were prepared for plasma sintering experiments. Tungsten filaments were inserted from one end of these rods to suspend them in the plasma.

2.2. Sintering

2.2.1. Conventional sintering

For conventional sintering studies, slip-cast and cold-pressed discs were placed on alumina plates. The sintering schedule consisted of a 2–3 h heat-up regime, a 4 h hold time at 1600 °C and furnace cooling. All samples were sintered in air. Some samples were sintered for 5 min at 1600 °C for comparison.

2.2.2. Plasma sintering

Rods were suspended from one end via W-filaments along the central axis of two concentric steel cylinders. Plasma sintering was carried out using the hollow-cathode discharge (HCD) method [6]. Upon reaching a 1.333 Pa vacuum, the plasma was generated by applying a 600–700 V d.c. voltage between the anode and cathode. The sample at the centre of two concentric cylinders (anode and cathode) was heated by electron bombardment and the hot plasma. The sample temperature was measured by an infrared pyrometer. Sintering was conducted in air plasmas at 1200–1300 °C, which was the highest temperature attainable in the system. Two samples per composition were sintered with a hold time of 4 min at the peak temperature.

2.2.3. Microwave sintering

A 2.45 GHz microwave source was used for sintering. Each sample was individually sintered in low density ZrO_2 insulation in air. Sample temperatures were measured using a fibre optic thermometer. Sintering was done at 1500–1600 °C for 5 min in air.

2.3. Characterization

Densities of sintered samples were measured, from at least two samples per group, using Archimedes' principle [1]. Scanning electron microscopy (SEM) was used for microstructural characterization. X-ray diffractometry (XRD) was utilized for phase determination. Microhardness was measured on polished surfaces by the Vickers indentation method, using loads of 500 g for 15 s. Samples with dimensions of roughly $4 \times 5 \times 15$–20 mm were prepared by a diamond saw. The indentation strength in bending (ISB) method [8] was used for fracture toughness evaluation. Indentation loads of 90 N were used to produce well-developed cracks.

3. Results

3.1. Sintering of MgO and MgO–10TiC

Consolidation behaviour was analysed by comparing the relative densities of each sample after completion of the sintering runs. Table I shows the final relative densities achieved by three different sintering methods. Relative densities of plasma-sintered samples were very low due to the low sintering temperatures and relatively slow sintering kinetics of MgO [4]. Although the bulk of plasma-sintered MgO had a low relative density, its exterior was sintered to quite high densities as suggested by the micrograph shown in Fig. 1. The average grain size was very small (1–2 μm), indicating that no grain growth occurred during plasma sintering.

TABLE I Fractional densities and mechanical properties of MgO and MgO–5TiC fabricated by various methods

Fabrication method	Material	Theoretical density (%)	H_V (GPa)	K_{Ic} ($MPam^{1/2}$)	K_{Ic} min/ K_{Ic} max	Number of samples[a]
Plasma sintering, 1300 °C, 4 min, vacuum	MgO_p	65.6	–	–	–	–
	MgO_p–10TiC	41.8	0.3	–	–	–
	MgO_{TG}	69.8	2.3	–	–	–
	MgO_{TG}–10TiC	48.0	1.0	–	–	–
Slip casting, conventional sintering, 1600 °C, 240 min, air	MgO_p	79.0	1.3	2.3	2.0/2.8	3
	MgO_p–10TiC	81.8	2.1	2.1	1.8/2.4	3
	MgO_{TG}	84.4	2.1	2.1	1.9/2.3	7
	MgO_{TG}–10TiC	92.8	2.9	2.7	2.5/2.9	6
Cold pressing, conventional sintering, 1600 °C, 240 min, air	MgO_p	90.1	3.4	–	–	–
	MgO_p–10TiC	92.3	4.0	2.6	2.5/2.7	2
	MgO_{TG}	88.5	2.6	2.2	1.9/2.4	6
	MgO_{TG}–10TiC	94.6	4.0	2.9	2.8/3.0	4
Cold pressing, conventional sintering, 1600 °C, 5 min, air	MgO_p	69.9	–	–	–	–
	MgO_p–10TiC	86.9	–	–	–	–
	MgO_{TG}	73.7	–	–	–	–
	MgO_{TG}–10TiC	93.1	–	–	–	–
Cold pressing, microwave sintering, 1500–1600 °C, 5 min, air	MgO_p	77.6	1.5	1.2	1.0/1.4	4
	MgO_p–10TiC	71.8	2.3	–	–	–
	MgO_{TG}	82.4	2.2	2.0	1.9/2.1	4
	MgO_{TG}–10TiC	77.3	3.2	1.7	–	1

[a] Number of samples used for K_{Ic} measurements.

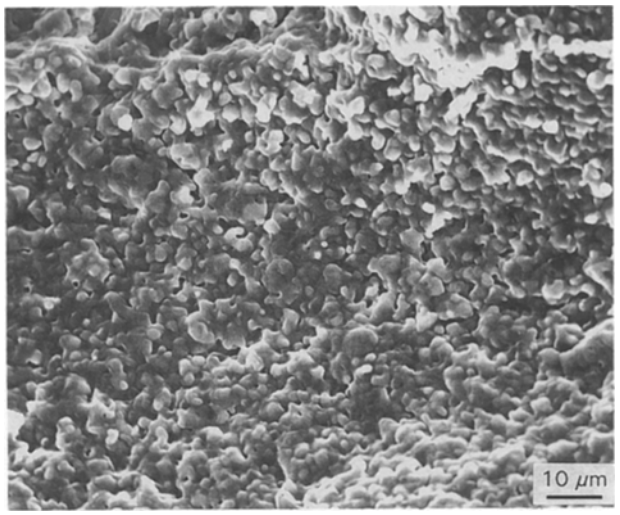

Figure 1 SEM micrograph of MgO_{TG} plasma sintered at 1300 °C for 4 min under 1.333 Pa vacuum.

Microwave sintering of MgO resulted in higher relative densities compared to those achieved by plasma or conventional sintering for the same hold times (4–5 min), as seen in Table I. However, lower densities were obtained compared to 4 h conventionally sintered samples. The higher relative densities of 5 min microwave-sintered MgO samples compared to 5 min conventionally-sintered MgO showed the positive effect of rapid heating or enhanced diffusion by microwaves [9]. Figs 2 and 3 show the microstructures of microwave-sintered samples. Microwave-sintered MgO_p exhibited fine grain size (mean diameter about 3 μm) and little porosity (Fig. 2a). The average grain size of microwave-sintered MgO_{TG} was larger than that of MgO_p (mean diameter about 7 μm), as shown in Fig. 3a. This difference probably stemmed from the higher sintering temperature used for these samples (1600 versus 1500 °C used in the former case) and/or from liquid-phase sintering [1]. Also, significantly coarser grains were observed in the case of MgO–TiC composites compared to MgO alone (Figs 2–6). This might have been due to the reaction of MgO and TiC resulting in Mg_2TiO_4. X-ray analysis indicated that Mg_2TiO_4 formed during the sintering of all MgO–TiC composites, although the relative intensity of Mg_2TiO_4 peaks were significantly lower in the case of plasma-sintered samples. It should be noted that relatively low temperatures (1200–1300 °C)

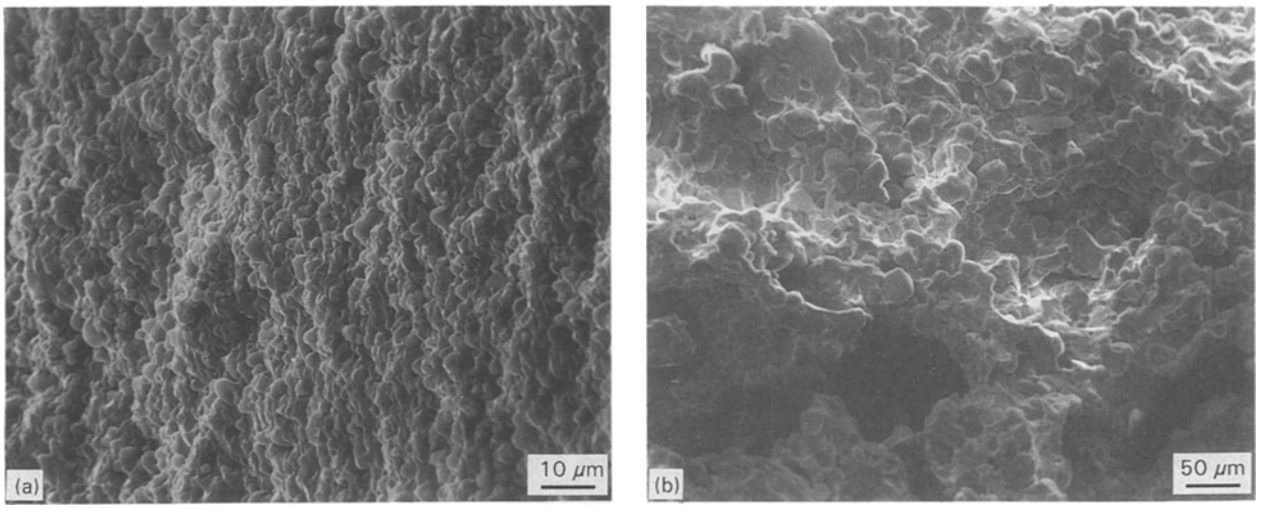

Figure 2 SEM micrographs of (a) MgO_p microwave sintered at 1500 °C for 5 min in air and (b) MgO_p–10TiC microwave sintered at 1600 °C for 5 min in air.

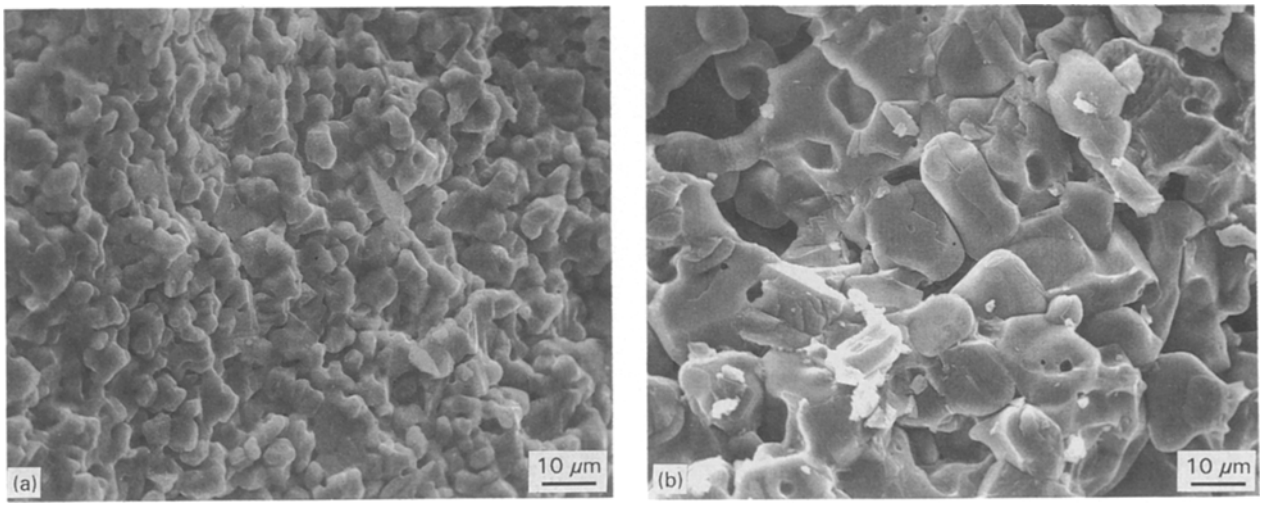

Figure 3 SEM micrographs of (a) MgO_{TG} microwave sintered at 1600 °C for 5 min in air and (b) MgO_{TG}–10TiC microwave sintered at 1500 °C for 5 min in air.

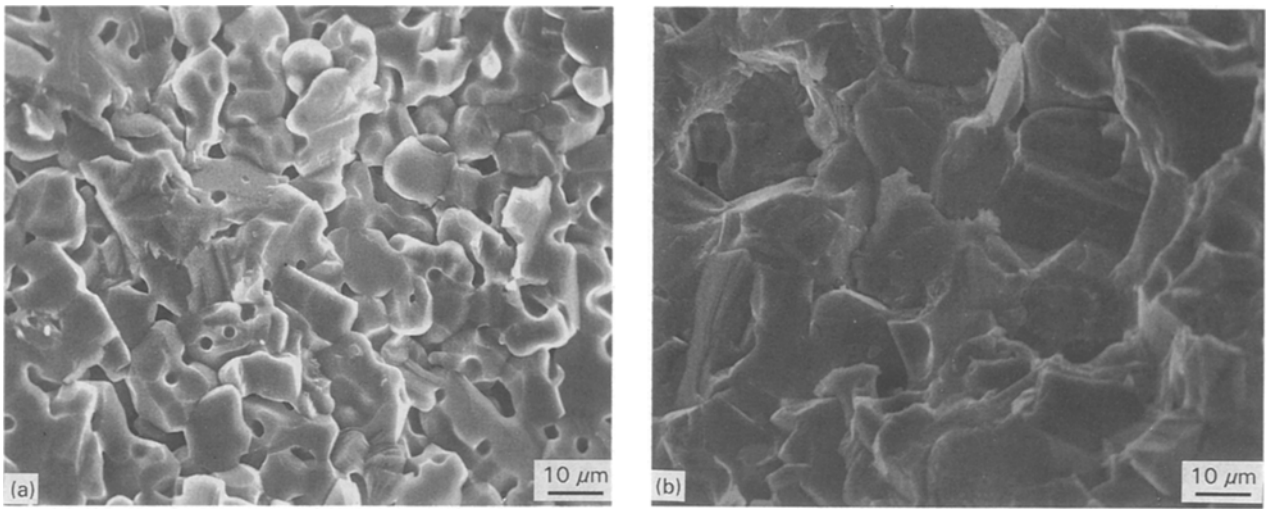

Figure 4 SEM micrographs of (a) MgO_{TG} and (b) MgO_{TG}–10TiC pressed and conventionally sintered at 1600 °C for 4 h in air.

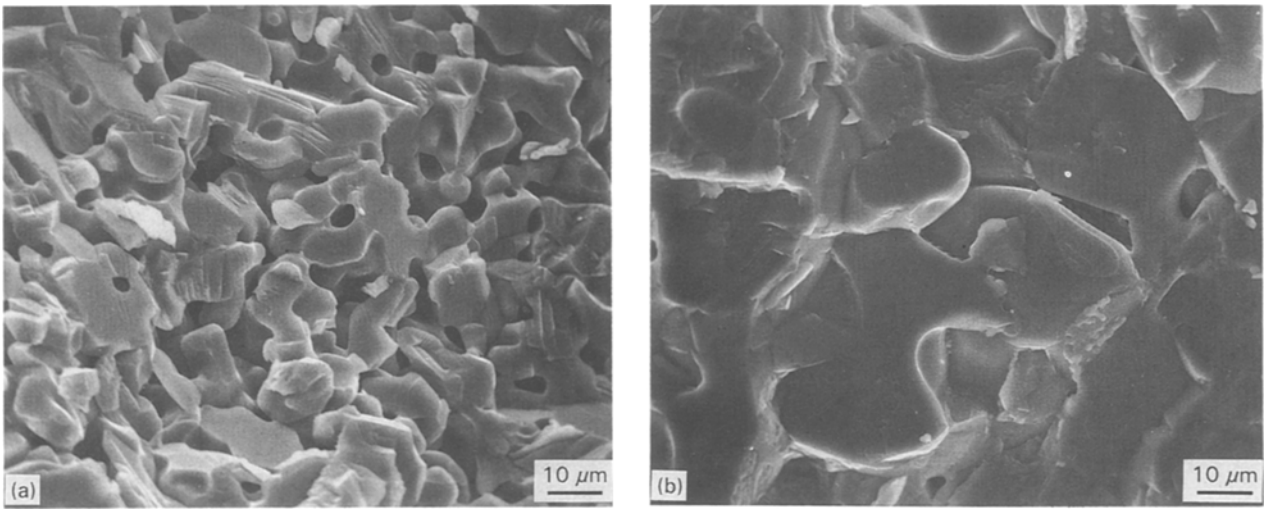

Figure 5 SEM micrographs of (a) MgO_{TG} and (b) MgO_{TG}–10TiC slip cast and conventionally sintered at 1600 °C for 4 h in air.

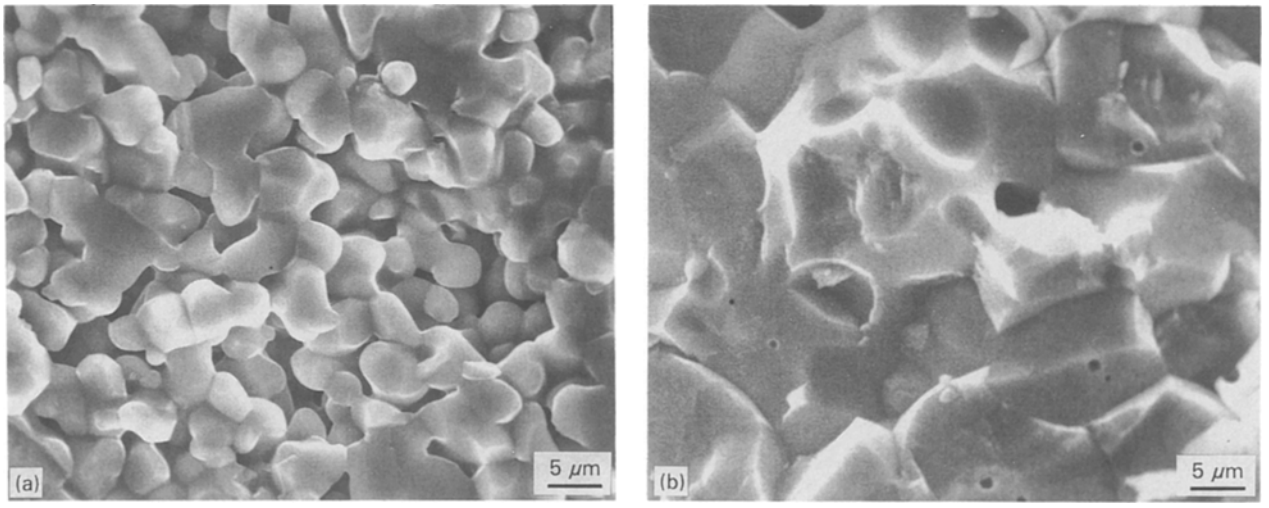

Figure 6 SEM micrographs of (a) MgO_p and (b) MgO_p–10TiC slip cast and conventionally sintered at 1600 °C for 4 h in air.

were used in plasma sintering, which may have been the cause of suppressed reaction. The absence of oxygen might have decreased the reaction rates as well. Formation of Mg_2TiO_4 in sintered MgO–TiC mixtures was observed as early as 1950 by Ueltz [10], although not in 10 vol % TiC containing samples but at higher TiC fractions (30 vol %). In Ueltz's study, sintering was performed in a He atmosphere, whereas

in the present study, excluding plasma sintering experiments, sintering was performed in air. It is suspected, therefore, that high oxygen partial pressures accelerated the reaction of MgO with TiC, probably through an initial TiO_2 layer formation [10]

$$TiO_2 + 2MgO \rightarrow Mg_2TiO_4$$

In the case of MgO–TiC composites, low bulk densities were achieved by microwave heating. The reason for low densities was the internal porosity that lead to a spongy structure, indicative of a gaseous reaction, most likely the oxidation of TiC according to [11]

$$TiC + 2O_2 \rightarrow TiO_2 + CO_2$$

A similar microstructure was observed in conventionally sintered MgO–50 vol % TiC composites due to severe reaction of MgO with TiC. The exterior of microwave-sintered MgO–TiC samples sintered to much higher densities, probably due to easier exit of the gaseous reaction product. Similarly, conventionally sintered MgO–10TiC composites did not exhibit such coarse-pored structures (Figs 4–6). This indicated that rapid heating of reactive MgO–TiC mixtures was disadvantageous due to the limited time of gas ejection to the exterior.

The results illustrated in Table I showed that MgO_{TG} and MgO_{TG}–10TiC samples were easier to sinter than MgO_p and MgO_p–10TiC samples. The reason for improved sinterability of MgO_{TG}-based samples was probably a higher contribution of liquid-phase sintering to the overall densification, due to the presence of impurities such as SiO_2, Fe_2O_3 and Al_2O_3. Liquid-phase sintering has previously been shown to improve the densification of MgO [12].

SEM micrographs of MgO and MgO–10TiC composites conventionally sintered for 4 h in air are shown in Figs 4–6. These micrographs exhibited that the addition of 10 vol % TiC to MgO decreased porosity while it led to grain coarsening. Comparison of the relative densities of conventionally sintered samples listed in Table I also indicated that MgO–10TiC composites attained higher relative densities than did monolithic MgO. This was a surprising result, since second-phase carbide particles are generally known to decrease the sinterability of a parent material, such as in the case of TiC, SiC or B_4C particle-reinforced Al_2O_3 [13]. In fact, plasma sintering results of the present study also pointed out that TiC limited the sinterability of MgO when their mutual reaction was suppressed. Table I shows that the addition of 10 vol % TiC limited the consolidation of MgO significantly in the case of plasma sintering. On the other hand, the fractional densities of conventionally sintered MgO–TiC composites were higher than those obtained in MgO alone, regardless of the green shaping method (dry-pressing or slip-casting) or purity (research grade or technical grade MgO), as shown in Table I. This result indicated that TiC or its reaction product (TiO_2 or Mg_2TiO_4) acted as a sintering aid in MgO during slow sintering in air. Although not stressed throughout the author's paper, Ueltz [10] also observed the positive effect of small TiC additions on sintering. Since the melting points of both TiO_2 and its interoxide compounds with MgO were all above 1600 °C [14], and since sintering was conducted at 1600 °C or below, liquid-phase sintering due to these phases did not seem to be the cause of improved sintering. Another study indicated that small amounts of TiO_2 addition improved the sintering kinetics of MgO considerably [15]. Thus the improved sintering rates could possibly be attributed to TiO_2 or Ti^{4+} ions rather than TiC.

Pressed samples reached higher fractional densities than slip-cast samples upon sintering (Table I). This difference was most likely due to the higher green densities of cold-pressed samples (30–35 versus 20–25% TD). It is generally accepted that higher powder compact densities led to higher sintered densities [16].

3.2. Mechanical properties

The mechanical properties of monolithic MgO and MgO–10TiC composites fabricated by various techniques are summarized in Table I. It can be observed that hardness improved with increasing relative densities, as expected. For example, the hardness of MgO_p increased from 1.3 to 3.4 GPa when its relative density increased from 79.0 to 90.1% TD by the application of cold-pressing instead of slip-casting. Similarly, the hardness of MgO_p–10TiC increased from 2.1 to 4.0 GPa with a density increase from 81.8 to 92.3% TD. The average hardness of MgO_p increased from 3.4 to 4.0 GPa and that of MgO_{TG} from 2.6 to 4.0 GPa with the addition of 10 vol % TiC. This increase may readily be explained by the improved fractional densities.

The hardness of microwave-sintered MgO_{TG}–10TiC was quite high when its relative density was taken into account. This discrepancy was due to the fact that the tabulated density came from the bulk sample, whereas the hardness was determined from the exterior region which was much less porous than the interior.

The fracture toughness of MgO was raised by TiC additions in the case of conventionally sintered samples. A useful number of samples from MgO–TiC composites could only be obtained in the case of these samples. The fracture toughness of slip-cast and sintered MgO_p remained essentially constant but that of MgO_{TG} increased slightly with TiC additions both in the case of slip-cast as well as pressed samples.

An important observation from fracture surfaces (Figs 4–6) was the change in fracture modes. In the case of monolithic MgO, the fracture mode was predominantly intergranular, as seen in Figs 4a, 5a and 6a. On the other hand, in the case of MgO–TiC composites, a significant portion of fracture occurred in the transgranular mode, as suggested by faceted grains in Figs 4b, 5b and 6b. Even in composites with considerable porosity, this behaviour was evident. The change of the fracture mode from intergranular to transgranular may have been due to the increased grain size, as suggested elsewhere [17]. Also, the fracture toughness improvement may have been related to the change in the fracture mode or to grain growth

upon TiC additions, or both. Toughening upon grain growth is well documented in the case of Al_2O_3 [18].

4. Conclusions

The following were found from the present study:

1. TiC reacted with MgO under the sintering conditions employed, yielding Mg_2TiO_4. Gaseous reaction products induced large pores during microwave heating of MgO–10TiC, but not in the case of slow heating. Large amounts (50 vol %) of TiC additions led to severe reaction and large pore formation even in the case of conventional sintering.
2. Plasma sintering of MgO at relatively low temperatures (1300 °C) and short times (4 min) did not produce satisfactory densification.
3. Ten vol % TiC addition increased the sinterability of MgO during conventional sintering in air. In contrast, it decreased the sinterability of MgO under vacuum (plasma sintering) where less reaction occurred. Improved sintering could be linked to the existence of TiO_2 during air sintering.
4. Microwave sintering of MgO was shown to be possible by indirect microwave heating. Microwave sintering of MgO yielded higher fractional densities compared to conventional sintering under the same sintering conditions.
5. The mechanical properties of MgO were improved by the addition of small amounts of TiC.

Acknowledgements

The present study was supported by Los Alamos National Laboratories under contract LANL 9XT 96721 R1 and is gratefully acknowledged. The authors express their appreciation to Drs J. D. Katz and R. D. Blake for microwave sintering of the samples.

References

1. D. W. RICHERSON, "Modern ceramic engineering" (Marcel Dekker, NY, 1982).
2. I. J. MCCOLM,"Ceramic science for material technologists" (Leonard Hill, London, 1983).
3. Y. IKUMA, W. KOMATSU and S. YAEGASHI, *J. Mater. Sci. Lett.* **4** (1985) 63.
4. R. MORRELL, "Handbook of properties of technical and Engineering ceramics, Part I" (Her Majesty's Stationary Office, London, 1985).
5. W. H. SUTTON, *Amer. Ceram. Soc. Bull.* **68** (1989) 376.
6. L. G. CORDONE and W. E. MARTINSEN, *J. Amer. Ceram. Soc.* **55** (1972) 380.
7. E. RICHERSON and D. W. RYKEWITCH, "Oxide ceramics" (Academic Press, Orlando, FL, 1985).
8. P. CHANTIKUL, G. R. ANSTIS, B. R. LAWN and D. B. MARSHALL, *J. Amer. Ceram. Soc.* **64** (1981) 539.
9. J. D. KATZ, *Ann. Rev. Mater. Sci.* **22** (1992) 153.
10. H. F. G. UELTZ, *J. Amer. Ceram. Soc.* **33** (1950) 340.
11. S. SHIMADA and M. KOZEKI, *J. Mater. Sci.* **27** (1992) 1869.
12. W. D. KINGERY, E. NIKI and M. D. NARASIMHAN, *J. Amer. Ceram. Soc.* **44** (1961) 29.
13. M. BENGISU and O. T. INAL, *Ceram. Int.* **17** (1991) 187.
14. "Phase diagrams for ceramists", edited by M. K. Reser (The American Ceramic Society, OH, 1964) p. 112.
15. G. K. LAYDEN and M. C. MCQUARRIE, *J. Amer. Ceram. Soc.* **42** (1959) 89.
16. T. S. YEH and M .D. SACKS, in "Ceramic transactions", Vol. 7, edited by C. A. Handwerker, J. E. Blendell and W. Kaysser (The American Ceramic Society, OH, 1990) p. 309.
17. R. W. RICE, in "Fractography of ceramic and metal failures", ASTMSTP 827, edited by J. J. Mecholsky Jr and S. R. Powell Jr (Am. Soc. Test. Mater., PA, 1984) p. 5.
18. P. L. SWANSON, C. J. FAIRBANKS, B. R. LAWN, Y. W. MAI and B. J. HOCKEY, *J. Amer. Ceram. Soc.* **70** (1987) 279.

Received 15 December 1992
and accepted 21 March 1994